Spectrochimica Acta Part A: Molecular and Biomolecular Spectroscopy 96 (2012) 332–339

Contents lists available at SciVerse ScienceDirect

Spectrochimica Acta Part A: Molecular and Biomolecular Spectroscopy

journal homepage: www.elsevier.com/locate/saa

Bis (trifluoromethyl) sulfone, $CF_3SO_2CF_3$: Synthesis, vibrational and conformational properties

M.E. Defonsi Lestard [a], L.A. Ramos [b], M.E. Tuttolomondo [a], S.E. Ulic [b,c], A. Ben Altabef [a,*]

[a] *INQUINOA-CONICET, Instituto de Química Física, Facultad de Bioquímica, Química y Farmacia, Universidad Nacional de Tucumán, San Lorenzo 456, T4000CAN Tucumán, Argentina*
[b] *CEQUINOR, Departamento de Química, Facultad de Ciencias Exactas, Universidad Nacional de La Plata, C.C. 962, 1900 La Plata, Argentina*
[c] *Departamento de Ciencias Básicas, Universidad Nacional de Luján, Rutas 5 y 7, 6700 Luján, Buenos Aires, Argentina*

HIGHLIGHTS

- ▶ The compound was characterized by vibrational spectroscopy and quantum chemical calculations.
- ▶ Quantum mechanical calculations indicate the possible existence of two conformers.
- ▶ The total potential energy was deconvoluted using a decomposition in terms of a Fourier expansion.
- ▶ Harmonic vibrational wavenumbers and a scaled force field were calculated.

GRAPHICAL ABSTRACT

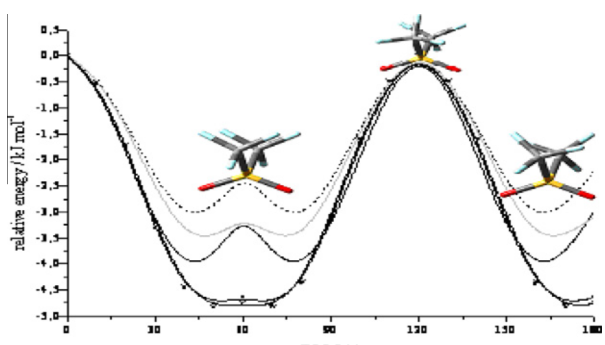

ARTICLE INFO

Article history:
Received 24 February 2012
Received in revised form 7 May 2012
Accepted 17 May 2012
Available online 26 May 2012

Keywords:
Quantum chemical calculations
Internal rotational barrier
Fourier-type expansion
Natural bond orbital analysis
Vibrational spectroscopy

ABSTRACT

Bis (trifluoromethyl) sulfone, $CF_3SO_2CF_3$, was obtained as a byproduct in the synthesis of $CF_3SO_2SCF_3$. The compound was characterized by infrared and Raman spectroscopy as well quantum chemical calculations. Quantum mechanical calculations indicate the possible existence of two conformers symmetrically equivalent with C_2 symmetry. The preference for the *staggered* form was studied using the total energy scheme and the natural bond orbital (NBO) partition scheme. Additionally, the total potential energy was deconvoluted using a sixfold decomposition in terms of a Fourier-type expansion, showing that the hyperconjugative effect was dominant in stabilizing the *staggered* conformer. Infrared and Raman spectra of $CF_3SO_2CF_3$ were obtained. Harmonic vibrational wavenumbers and a scaled force field were calculated, leading to a final root mean-square deviation of 7.8 cm^{-1} when comparing experimental and calculated wavenumbers.

© 2012 Elsevier B.V. All rights reserved.

Introduction

The sulfonyl group found large applications in organic and medicinal chemistry, both in sulfonamides, popular as a solid group for the protection of amines, and sulfones [1]. Frequently, sulfones in synthetic systems are inserted to help certain transformations. The use of sulfones, as an auxiliary group, remains a significant synthetic strategy, especially for the formation of carbon–carbon double bond [2,3]. This functional group can change the polarity of the molecule, as an electron-withdrawing group, to stabilize carbanions or as a leaving group. In recent years the use of sulfones as intermediates in the total synthesis of many natural products has become a classic. The molecular structures of a relatively large series of sulfone derivatives have been determined. For example, the electron diffraction analysis (GED) resulted in C_2 symmetry for the $CCl_3SO_2CCl_3$ molecule, with the two CCl_3 groups rotated 12° in the opposite direction of the C_{2v} position, and tilted away from each about 5° [4].

* Corresponding author. Tel.: +54 381 4311044; fax: +54 381 4248169.
E-mail address: altabef@fbqf.unt.edu.ar (A. Ben Altabef).

1386-1425/$ - see front matter © 2012 Elsevier B.V. All rights reserved.
http://dx.doi.org/10.1016/j.saa.2012.05.049

Moreover, the experimental determination of the geometric parameters of $CF_3SO_2CF_3$ by GED in the gas phase was previously reported by Oberhammer [5] in 1981. The resulting symmetry for the molecule is C_2 with ∠FCF of 109.6° and an effective torsional angle of 14.1°.

In addition, structural and conformational properties of several sulfones of the type CF_3SO_2R with R = F, OH, NH_2, CH_3 [6] were previously studied in this laboratory.

In this work a complete analysis of the infrared and Raman vibrational recorded spectra for $CF_3SO_2CF_3$ is presented. The harmonic vibrational wavenumbers and scaled force fields are also calculated for this molecule and compared with related compounds [6].

Additionally, the geometric parameters obtained by quantum chemical calculations with different basis sets are compared with experimental data and with results of other sulfones.

Besides, the energy of the system, related to the internal rotation around the C–S bond, is calculated using several computational approaches and fitted to the sixfold Fourier-type expansion. This methodology allowed the characterization of the potential function nature, which explains the preferred conformation of this molecule. The study is complemented by a natural bond orbital (NBO) analysis to evaluate the significance of the hyperconjugative interactions and electrostatic effects on such conformation.

Experimental and theoretical methods

Synthesis

Bis (trifluoromethyl) sulfone, $CF_3SO_2CF_3$, was obtained as a byproduct in the synthesis of $CF_3SO_2SCF_3$, which was carried out following the literature procedure [7] with some modifications [8]. The reaction products were separated by trap to trap distillation. Pure $CF_3SO_2CF_3$ was isolated as a colorless liquid in the −95 °C trap.

Infrared and Raman spectroscopy

The infrared spectrum for $CF_3SO_2CF_3$ in the gas phase was recorded in the 4000–400 cm^{-1} range (spectral resolution of 2 cm^{-1}) at room temperature using a LUMEX Infra LUM FT-02 spectrometer. An IR glass cell 200 mm optical path length and 0.5 mm thick Si windows was used to obtain gas phase spectra. Raman spectra of the liquid at room temperature with a resolution of 2 cm^{-1} were obtained using a Bruker IFS 66 spectrometer (spectral resolution 4 cm^{-1}). The 1064 nm radiation line of an Nd/YAG laser was used for excitation. The liquid sample was handled in flame-sealed tubes (4 mm o.d).

Computational details

Calculations were performed with the Gaussian 03 [9] package. Potential energy curves were calculated at the B3LYP [10–12] level using the 6-31G(d), 6-311G(d), 6-311+G(d), 6-311G(3df) and 6-311+G(3df) [13–17,10] basis sets, and two mimima symmetrically equivalent were identified by rotating the S–C bond. Furthermore, the influence of the level was tested by using the functional mMPW1PW91 [18] with the 6-311+G(d) basis set. The *ab initio* Møller–Plesset second order perturbations method (MP2) [19] was employed in the same way, using the 6-311G(3df) and 6-311+G(3df) basis sets. All calculations were performed in such a way, that only the given torsion (FCSC) was fixed and other parameters were allowed to relax. The total energy curve was constructed in steps of 10° using default convergence criteria as implemented in Gaussian 03.

Geometry optimizations for $CF_3SO_2CF_3$ were performed at the MP2-31G(d) with 6-311G(d), 6-311+G(d) and 6-311G(3df) basis sets and DFT (B3LYP, mPW1PW91) approximation using 6-311G(3df) the basis set.

Additionally we compared the theoretical structures and conformations of $CF_3SO_2CF_3$ with the theoretical and experimental results previously obtained for $CCl_3SO_2CCl_3$, $CBr_3SO_2CBr_3$ [20] and $CH_3SO_2CH_3$ [4].

A natural bond orbital (NBO) calculation was performed at the B3LYP/6-311+G(d) level using the NBO 3.0 [21] code as implemented in the Gaussian 03 package.

A harmonic force field in Cartesian coordinates calculated at the B3LYP/6-311+G(d) level was transformed to a set of natural internal (local symmetry) coordinates *via* the B matrix using a standard program. The scaled quantum mechanical (SQM) force field was obtained using the scheme outlined by Pulay et al. [22], in which the diagonal force constants are multiplied by scale factors f_i, f_j,... and the corresponding interaction constants are multiplied by $(f_i \cdot f_j)^{1/2}$, thus adjusting the scale factors to reproduce the experimental wavenumbers as well as possible. An initial set of scale factors was refined to fit the calculated wavenumbers for the experimental data. No empirical correction of the theoretical geometry was used. The potential-energy distribution was then calculated with the resulting SQM force field. The force field for the C_2 conformation, scaling and determination of the potential-energy distribution were performed with the FCARTP program [23]. The atomic displacements given by the Gaussian 03 program for each vibrational mode were used to understand the nature of the molecular vibrations qualitatively. Hence, the corresponding data were represented graphically using the GaussView program [24].

Results/discussion

Quantum chemical calculations

The potential function for internal rotation around the C–S bond was derived by structure optimizations of the C_2 symmetry conformer at fixed FCSC dihedral angles. Potential functions obtained with several combinations of method and basis sets are shown in Fig. 1.

Minima occur at 40° and 80°, which are symmetrically equivalent (*enantiomers*). In these structures the CF_3 groups are allowed to deviate from the *staggered* position (with each other and with the SO_2 group), so that the molecule belongs to C_2 symmetry group. The curves possess two maxima, TS1 with *Cs* symmetry and TS2 with C_{2v} symmetry. The both conformers have imaginary wavenumbers. The higher energy transition state (TS1) shows both CF_3 groups staggered between them and with respect to the S═O bonds, whereas both CF_3 groups are eclipsed between them and staggered with respect to the S═O bonds in the lower energy transition state (TS2) (Fig. 2).

Predicted and relative energies for the C_2 conformer and the two transition states are collected in Table S1. This table shows that when the set of basis functions is extended, the stability of the *staggered* conformer increases and the energy of the TS1 transition state decreases. However, it is interesting to note that the energy of TS1 is lower at the B3LYP/6-311G(3df) level than at the B3LYP/6-311G+(3df) combination.

The geometries of the C_2 conformer were fully optimized including wavenumber calculations with the MP2 method using 6-31G(d), 6-311G(d), 6-311+G(d) and 6-311G(3df) basis sets and DFT (B3LYP, mPW1PW91) approximation with the 6-311G(3df)

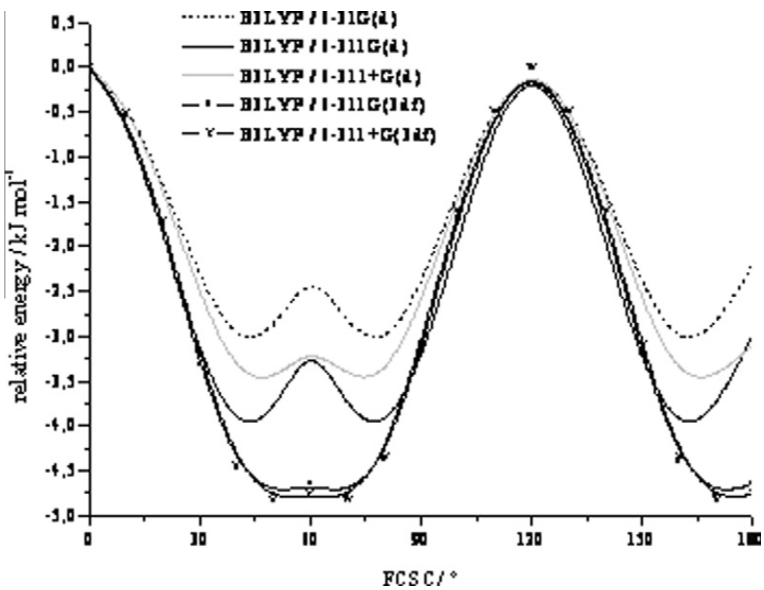

Fig. 1. Torsional potential energy curves for internal rotation around the C–S bond in $CF_3SO_2CF_3$ calculated at B3LYP level of theory with different basis sets.

Fig. 2. Optimized structures of the *staggered* conformation and the two transition states calculated at the B3LYP.level of theory.

basis set. The geometric parameters are calculated in this work and experimentally determined by Oberhammer [5] as shown in Table 1. The MP2/6-311(3df) combination produces a bond distances close to the experimental values. However, the values of the bond angles are better reproduced with B3LYP/6-311(3df) level. The most sensitive parameter to the method resulted the C–S bond, which was shortened by 3.9–3.4 pm upon replacing the DFT method with the MP2 method. Furthermore, the C–S and S=O bonds were shortened by 2.0 and 1.7 pm upon replacing the 6-311(d) basis set with 6-311(3df), respectively, showing to be sensitive to the change of basis set. The minor RMSD was obtained with the MP2/6-311G(3df) for the bond distances and B3LYP/6-311G(3df) for the bond angles.

The study of the nature of the rotational barrier of the FCSC torsion, in terms of hyperconjugative, steric and electrostatic interactions will give us an insight into the reasons for the relative stability of the C_2 conformer [25–29]. The potential energy surface for the target torsion angle was calculated in 10° steps in the range 0–180° allowing to relax all other geometrical parameters. The energy profiles were fitted to a sixth-order Fourier expansion:

$$V(\theta) = \sum_{i=1}^{6} \frac{1}{2} V_{iN}\, (1 - \cos\ iN\theta)$$

where θ is the angle of rotation and N, the symmetry number, is equal to 1. No contributions to torsional energies from zero-point energy were taken into account.

The decomposition of the total energy function and the analysis of the different terms V_i are a simple way of analyzing the stabilization of different conformations in molecular systems. Table S2 lists the six V_i terms calculated for $CF_3SO_2CF_3$ at the B3LYP/6-311+G(d) level. The large V_3 and V_6 values are the main contributions to the rotational barrier, while $V_5 > V_1 > V_2 > V_4$ are less significant when deconvoluting the potential energy curve. Fig. 3 shows the Fourier decomposition for the potential energy function at the B3LYP/6-3116+G(d) basis set. The V_3 term is large and negative, showing

Table 1
Calculated and experimental geometrical parameters for $CF_3SO_2CF_3$.

	GED[a]	B3LYP	mPW1PW91		MP2	
		6-311G(3df)	6-311G(3df)	6-311G(d)	6-311(3df)	6-311+G(d)
Distances (pm)						
C–F	132.1	132.4	131.6	132.7	132.0	132.5
S=O	142.4	142.9	142.2	144.4	142.7	144.5
S–C	185.8	189.3	187.2	187.4	185.4	188.0
RMSD		4.14	0.87	2.30	0.09	3.1
Angles (°)						
FCF	109.6	109.8	109.8	109.7	107.0	109.8
OSO	122.9	123.8	123.8	125.3	124.5	124.8
CSC	102.2	102.2	102.4	100.0	100.8	101.1
CSO	107.5	107.2	107.2	107.1	107.3	107.1
RMSD		0.24	0.98	2.71	3.8	1.3
RMSD total		4.40	1.89	5.02	3.9	4.4

[a] Ref. [5].

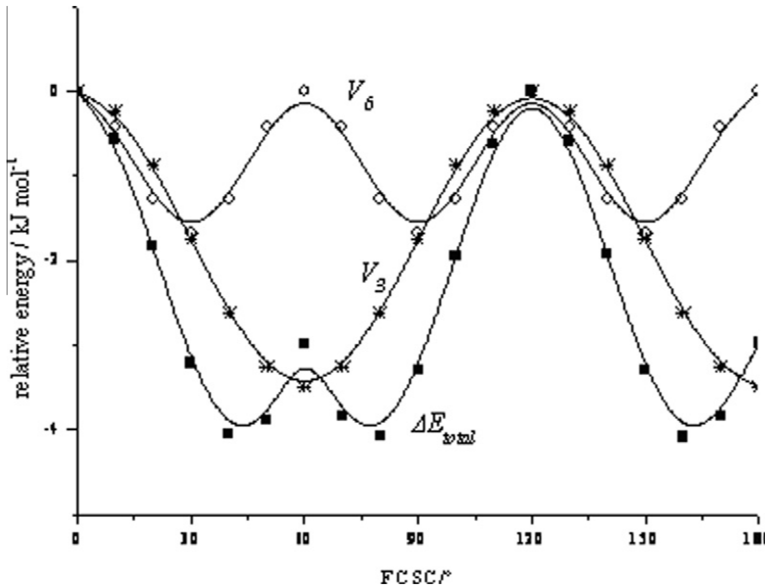

Fig. 3. Fourier decomposition of the potential function $V(\theta)$ for $CF_3SO_2CF_3$ calculated using the B3LYP method with the 6-311+G(d) basis set.

that there is a strong preference for the 60° and 180° geometry (TS2) (symmetrically equivalent) over 0° geometry (TS1). The V_3 term is associated with unfavorable bond–bond eclipsing interactions between the CF_3 groups, exhibiting a threefold periodicity for a torsion involving sp^3-hybridized sulfur atoms while the behavior of the V_6 term is less favorable for both transition states. The balance between the V_3 and V_6 terms contributed to the stabilization of the *staggered* form. The absolute values of V_3 and V_6 gave the barrier energy and form, respectively.

In order to confirm the contributions of the different terms in the Fourier decomposition the analysis of the barrier was carried out in terms of electrostatic interactions of attraction and repulsion based on the partition offered by the equation:

$$\Delta E = \Delta E_{nn} + \Delta E_{en} + \Delta E_{ee} + \Delta E_{k}$$

where ΔE is the total energy change between structures of different geometries, ΔE_{nn} is the energy change for nuclear repulsion, ΔE_{en} electron–nuclear attraction, ΔE_{ee} electron repulsion and ΔE_{k} is the kinetic energy. This equation describes the total energy change as the sum of all potential and kinetic contributions. The ΔE_{en} term stabilizes the *staggered* conformer following the same trend V_6, whereas ΔE_{ee} and ΔE_{nn} show a preference for the transition state (Fig. S1).

The detail in Fig. 4, where the variation of the dipole moment as a function of the FCSC torsion follows the same form as ΔE_{ne}.

The natural bond orbital (NBO) analysis [21] has frequently been used in the evaluation of the anomeric effect and the origin of the internal rotation barrier. The NBO analysis allows us to estimate the energy of the molecule with the same geometry, but in the absence of the electronic delocalization. Moreover, only the steric and electrostatic interactions through the E_{Lewis} term were taken into account.

Following this scheme, the energy barrier $\Delta E_{barrier}$ can be written as a function of bond strength, hyperconjugation and steric repulsion:

$$\Delta E_{barrier} = \Delta E_{Lewis} + \Delta E_{deloc} = \Delta E_{struct} + \Delta E_{exc} + \Delta E_{deloc} \quad (1)$$

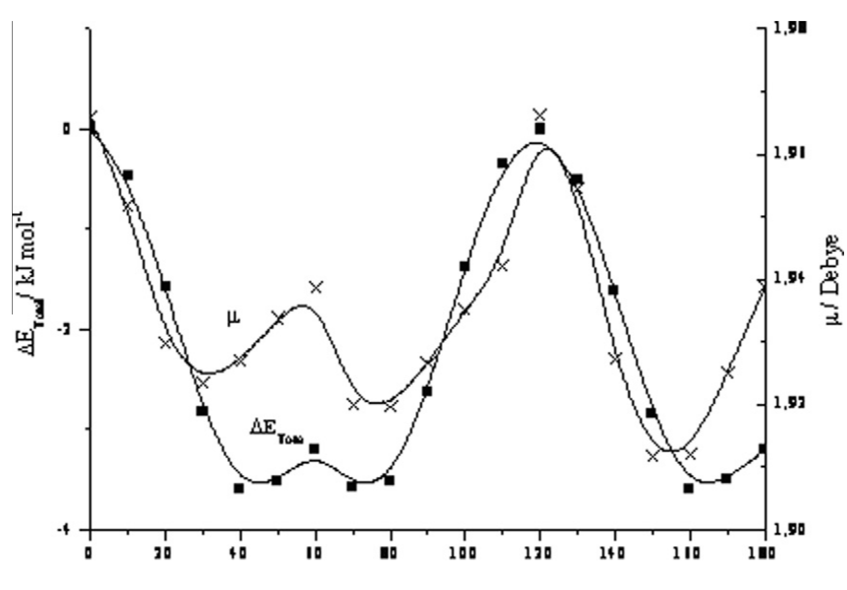

Fig. 4. Variation of the molecular dipole moment as function of the FCSC dihedral angle calculated at B3LYP/6-311+G(d) level.

Table 2
Relevant hyperconjugative interactions and dipole moment for $CF_3SO_2CF_3$ calculated at B3LYP/6-311+G(d).

	$LP^a(\sigma)O \rightarrow \sigma^*C–S$	$LP^a(\pi)O \rightarrow \sigma^*C–S$	μ^b
TS1	20.24	4.11	1.94
Staggered conformer	24.73	2.58	1.92
TS2	18.5	8.56	1.97

[a] Energies in kJ mol^{-1}.
[b] Debye.

where ΔE_{struct} takes into account Coulombic and bond-energy changes in the classical structure, ΔE_{exc} (known as the Pauli exchange (or steric) repulsion energy) accounts for the non-Coulombic energy changes arising from the Pauli exclusion principle, and ΔE_{deloc} describes the hyperconjugative stabilization.

Table 2 presents the contributions from the localized electron density (E_{Lewis}) and the delocalized electron density (E_{deloc}) for the rotation barrier about the S–C bond at the B3LYP/6-31+G(d) level. This table shows that the electronic delocalization is decisive for the energetic preference; its minima correspond to the *staggered* conformer. The Lewis energy is maximum for the TS1 state and minimum for TS2.

Important conclusions arise from the analysis of the dipole moments. It is important to stress that the original electrostatic interpretation of the anomeric effect is related to the dipole–dipole interaction between the C–S bond and the lone pairs of the oxygen atom. As can be seen in Table 3, the dipole moment of the *staggered* conformer is smaller than that of the TS1 and TS2 conformers. It thus seems that the anomeric effect can be rationalized in terms of the electrostatic theory as well as by the interactions between the lone pair of the O atom and the C–S antibonding orbital, lp(O) → σ*(C–S).

In Fig. S2 the torsional barrier for rotation about the C–S bond for $CF_3SO_2CF_3$, $CCl_3SO_2CCl_3$ $CBr_3SO_2CBr_3$ [20] and $CH_3SO_2CH_3$ [4] is presented. The curves of the first three molecules have very similar shapes, being the main difference the height of the barrier, which decreases with the increase of the electronegativity of the CX_3 group. Each curve has a minimum related to a *staggered* orientation ($\phi \cong 40°$) and two maxima for 0° (TS1) and 180° (TS2). The behavior of $CH_3SO_2CH_3$ is slightly different; it shows only one transition state, TS1 (0°), and has two equivalent minima related to the *eclipsed* conformation (60° and 180°).

Vibrational analysis

The bands observed in the infrared and Raman spectra of $CF_3SO_2CF_3$ were assigned by comparison with related molecules [6,8]. The molecule possesses C_2 symmetry and the 27 fundamental modes are all IR and Raman actives. The infrared spectrum of $CF_3SO_2CF_3$ in gaseous phase is shown in Fig. 5 together with the calculated one (B3LYP/6-31+G (d)) and the Raman spectrum of the liquid in Fig. 6. The observed IR and Raman wavenumbers are reported in Table 4.

Table 3
Lewis energy (E_{Lewis}) and the hyperconjugation energy (E_{deloc}) contribution to the rotation around the FCSC torsion angle for $CF_3SO_2CF_3$.

Structure	E_{Lewis} (au)	ΔE_{Lewis} (kJ mol^{-1})	E_{deloc} (au)	ΔE_{deloc} (kJ mol^{-1})
TS1	−1222.49575	0	−1.58876	0
Staggered conformer (1)	−1222.50308	−19.22	−1.58280	15.62
TS2	−1222.50631	−27.67	−1.57942	24.45
Staggered conformer (2)	−1222.50298	−18.97	−1.58287	15.44

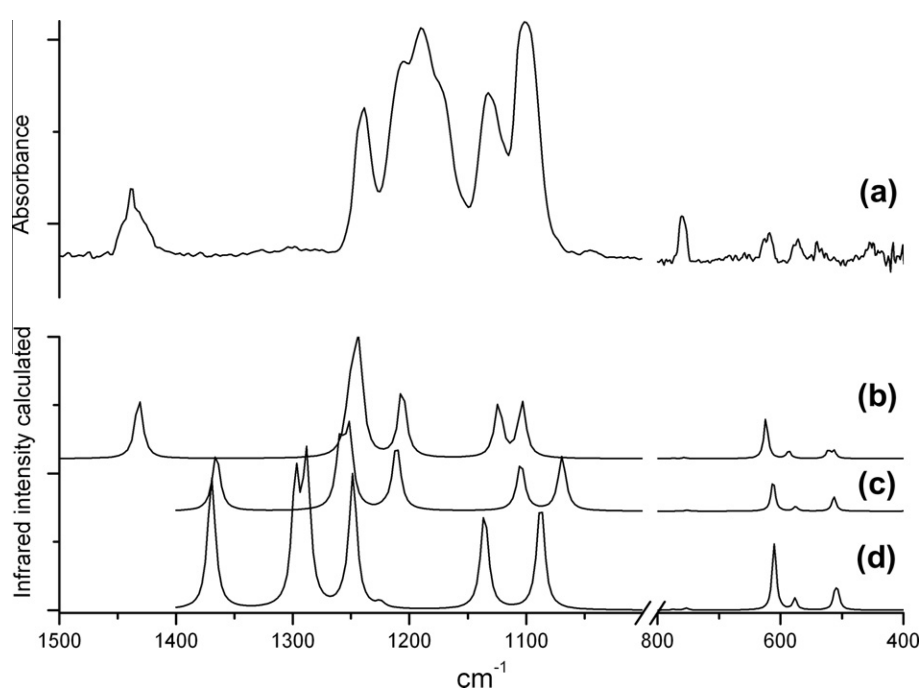

Fig. 5. Infrared spectra of $CF_3SO_2CF_3$ (a) the gas phase (path length: 20 cm, pressure: 4 Torr, resolution: 2 cm^{-1}); and the B3LYP calculated spectra with the following basis sets: (b) 6-311G(3df), (c) 6-311(d), (d) 6-31G(d).

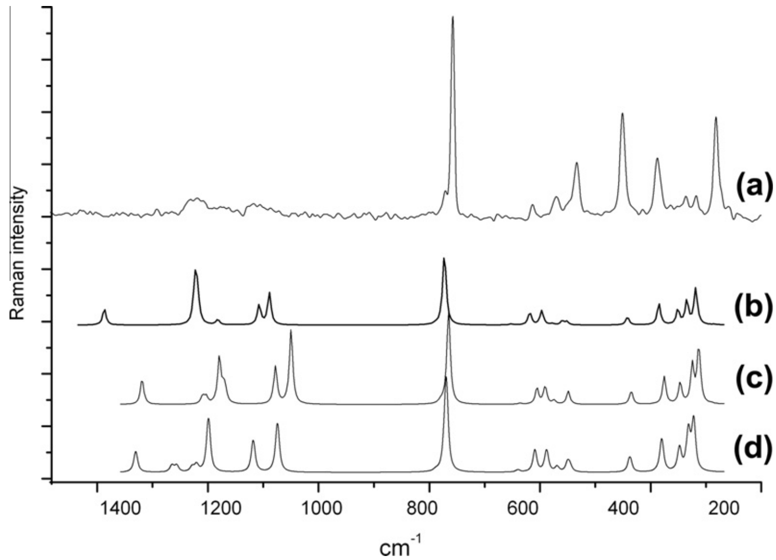

Fig. 6. (a) Raman spectra of liquid $CF_3SO_2CF_3$ at room temperature (resolution: 4 cm^{-1}); and the B3LYP calculated spectra with the following basis sets: (b) 6-311G(3df), (c) 6-311(d), (d) 6-31G(d).

Table 4
Experimental, calculated wavenumbers, intensities and assignments of the fundamental vibrational modes of $CF_3SO_2CF_3$.

Mode	Experimental		Calculated				Assignment
	Infrared[a] Gas (4 Torr)	Raman[b] Liquid (R.T.)	B3LYP/ 6-31G	SQM[c]	IR Intensity[d]	Raman Activity[e]	
ν_1	1438 m	1493 (17)	1370	1422	278.6	3.38	νa SO_2
ν_2	1244	1231 (16)	1297	1249	262.73	1.06	νa CF_3
ν_3	1238 s	1219 (14)	1288	1241	1288	1241	νa CF_3
ν_4	1238 s	1219 (14)	1256	1236	1256	1236	νa CF_3
ν_5	1205 s	1208 sh	1249	1200	1249	1200	νa CF_3
ν_6	1190 vs	1171 (10)	1225	1199	1225	1199	νs CF_3
ν_7	1132 s	1119 (12)	1136	1136	206.0	4.95	νs CF_3
ν_8	1101 vs	–	1088	1103	229.96	7.56	νs SO_2
ν_9	770	771 (18)	774	780	1.85	0.22	δs CF_3
ν_{10}	760 m	757 (100)	753	755	4.34	13.56	δs CF_3
	626 vw	–					
ν_{11}	618 w	613 (12)	610	614	140.20	0.31	ω SO_2
	578 sh						
ν_{12}	572 w	571 (15)	577	581	23.79	2.99	δ SO_2
ν_{13}	550 sh	–	554	555	0.19	2.99	δa CF_3
ν_{14}	532 vw	534 (31)	533	532	0.03	0.70	δa CF_3
ν_{15}	512 sh	–	511	511	33.42	1.29	δa CF_3
ν_{16}		–	506	505	29.39	0.75	δa CF_3
	416 vw	451 (55)414 (10)					
	401 vw	–					
ν_{17}	–	388 (31)	388	398	5.04	2.01	ρ SO_2
ν_{18}	–	335 (16)	325	334	1.13	4.26	ρ CF_3
	–						
ν_{19}	–	318 (16)	289	300	0.01	2.97	$\tau\omega$ SO_2
ν_{20}	–	281 (53)	271	278	2.01	5.04	νa CSC
ν_{21}	–	274 h	260	271	0.02	6.40	νs CSC
ν_{22}	–	225	225	238	8.77	0.01	ρ CF_3
ν_{23}		200	186	192	4.95	0.10	ρ CF_3
ν_{24}		200	180	184	0.01	0.46	ρ CF_3
ν_{25}			108	110	0.26	0.23	δ C–S–C
ν_{26}			43	41	0.21	0.00	CF_3 torsion
ν_{27}			40	38	0.04	0.00	CF_3 torsion
RMSD (cm^{-1})			24.16	7.8			

For symmetry coordinate descriptions see Table S3 (Supplementary material).
[a] Band intensities: vs, very strong; s, strong; m, medium strong; w, weak; vw, very week and sh, shoulder.
[b] Relative intensities in parentheses.
[c] From Scaled Quantum Mechanics force field. Wavenumbers values in cm^{-1}.
[d] Infrared intensities in km mol^{-1}.
[e] Raman activities in $Å^4/amu^{-1}$.

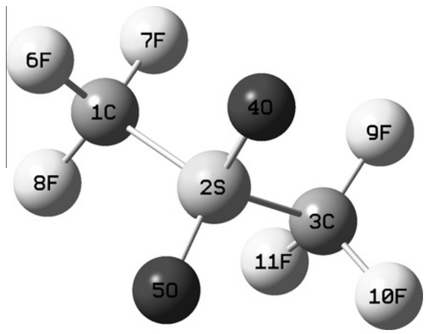

Fig. 7. Calculated molecular structure, atom numbering and definition of internal coordinates for $CF_3SO_2CF_3$.

Band assignments

SO_2 modes

The medium intense band located at 1438 cm^{-1} in the infrared spectrum was assigned to the SO_2 antisymmetric stretching mode which appears at 1422 and 1456 cm^{-1} in the IR spectra of $CF_3SO_2SCF_3$ [8] and CF_3SO_2OH [6], respectively.

The SO_2 symmetric stretching mode is predicted in the region of 1250–1100 cm^{-1}. Taking into account the calculated wavenumbers, the intense band in the infrared spectrum at 1101 cm^{-1} is assigned to the SO_2 symmetric stretching mode. The bands at 571 and 572 cm^{-1} in the infrared and Raman spectra, respectively, are originated by the deformation of the SO_2 group. This assignment was made taking into account the same mode in related molecules. The modes corresponding to the vibrations of the whole SO_2 group at 618 (SO_2 wagging), 388 (SO_2 rocking) and 318 cm^{-1} (SO_2 twisting) are supported by the theoretical calculations and by comparison with similar compounds.

The predicted wavenumber for the CSC deformation, associated with the movements of the SO_2 group, resulted 104 cm^{-1} and could not be observed in the vibrational spectra.

Trifluoromethyl modes

Five bands can be observed in the IR spectra which are assigned to the stretching of the CF_3 groups. The assignments of the CF_3 modes were difficult because the modes of both CF_3 groups were very mixed. The bands at 1244, 1238 and 1205 cm^{-1} are attributed to the four antisymmetric stretching modes of both CF_3 groups.

The CF_3 symmetric stretching modes of the two CF_3 groups are attributed to the bands at 1190 and 1132 cm^{-1}. The bands at 771 and 757 cm^{-1} in the Raman spectrum are associated to the symmetric deformation of the CF_3 groups. The calculated $\Delta\nu$ for these modes is 24 cm^{-1} and the observed $\Delta\nu$ resulted 26 cm^{-1}. The CF_3 antisymmetric bending modes were assigned to the infrared band at: 550, 532, 512 (this last wavenumber is assigned to two modes), according to the related molecules [6].

The bands at 335, 225, 200 cm^{-1} in the Raman spectrum are attributed to the CF_3 rocking modes, according to related sulfones, in which the corresponding modes showed up in the (333–322) and (204–196) cm^{-1} regions.

C–S stretching mode

The Raman band at 281 cm^{-1} and the shoulder at 274 cm^{-1}, are assigned to the C–S–C antisymmetric and symmetric modes, respectively. These vibrations appeared, in similar compounds, in the region of around 300 cm^{-1}.

Torsional modes

Two modes are predicted for the torsional rotation of both CF_3 groups, at 43 and 40 cm^{-1}. They could not be observed because of measurement range of the Raman spectrophotometer.

Force constants calculations

The Cartesian force field for $CF_3SO_2SCF_3$ resulting from the B3LYP/6-31G(d) calculations was transformed to the set of non-redundant, natural coordinates defined in Table S3 (See Fig. 7 for atom numbering and internal coordinates definition). Such coordinates take into account the local symmetry around the C atoms and follow the proposals of Fogarasi et al. [30]. The resulting force field was subsequently scaled using the scheme proposed by Pulay et al. [22] (see 'Computational details'). All of the initial scale factors were taken as the unit for all modes and were subsequently modified by a least squares procedure to obtain the best fit to the experimental wavenumbers, as shown in Table S4.

The same weight in the adjustment was assigned to all vibrational frequencies, and no empirical correction was used for the theoretical geometry. The resulting scaled quantum mechanical (SQM) force field was used to calculate the potential energy distribution for the molecule. The final RMSD is shown in Table 4.

The SQM force field was used to calculate the internal force constants shown in Table 5, and compared with the equivalent values for related molecules. This table shows that when the electronegativity of the X group decreases, the force constant of the C–S bond decreases, which is in agreement with the increase of the bond distance [6]. However, when the force constant of the S–X bond increases, an increase in the bond distance is observed.

This behavior could be understood by the decrease in X electronegativity along the series favoring the delocalization of the lone pairs of electrons on X in the SX bond and strengthening the bond, which explains the increase of the force constants along the CF_3SO_2F, CF_3SO_2OH, $CF_3SO_2NH_2$ series. It would also agree with the reduction of the force constant of the S–X bond in $CF_3SO_2CH_3$ and $CF_3SO_2CF_3$, for which the C atom has no free electrons.

Table 5
Force constants in internal (valence) coordinates for $CF_3SO_2CF_3$ and related molecules.

Force constants[a]	$CF_3SO_2CF_3$ [b]	CF_3SO_2F[c]	CF_3SO_2OH[c]	$CF_3SO_2NH_2$[c]	$CF_3SO_2CH_3$[c]
k_f[C(1)–F]	6.37	6.16	6.05	5.98	5.90
k_f[C–S]	2.62	3.02	3.08	3.14	2.89
k_f[S–X]	2.62	4.67	4.98	6.23	3.06
k_f[S=O]	10.46	10.97	10.54	10.17	9.93
k_f[O=S=O]	0.88	1.11	1.12	1.11	1.14
k_f[O=S–C(1)]	0.85	0.98	1.01	1.05	1.09
k_f[O=S–X(3)]	0.85	1.24	1.29	1.30	1.06
k_f[C–S–C]	1.25	0.95	0.96	1.03	0.99

[a] Units in mdyn $Å^{-1}$ (for stretches and stretch-stretch interactions) and mdyn Å rad^{-2} (for angle bendings).
[b] This work.
[c] Ref. [6].

However, the stretching force constant of the S–X bond results higher for $CF_3SO_2CH_3$ than for $CF_3SO_2CF_3$, contrary to expectations, because the S–X bond distance is 8.7 pm shorter for $CF_3SO_2CH_3$. This can be attributed to the electronic delocalization effect of the electron lone pairs on the F atom of the CF3 group.

Fig. S3, A and B, shows the variation of the S=O bond force constant, depending on the electronegativity of the X atom and the interaction energy LPO → σ*S=O for the CF_3SO_2X (X = CF_3, OH, NH_2, CH_3) species, respectively. The force constant of the S=O bond increases with the increasing electronegativity of the substituent X and with the decrease of the interaction energy LPO → σ*S=O. Fig. S3, C, shows the relationship between the electronegativity of the X atom and the interaction energy LPO → σ*S=O.

Conclusions

The optimized molecular geometry and conformations for bis (trifluoromethyl) sulfone are calculated using MP2 and DFT techniques and different basis sets. The structural results showed that the preferred form is the *staggered* (C_2). The decomposition of the potential-energy function as a Fourier expansion and the analysis of different terms (V_i) were useful to analyze the relative stabilities of different conformations of this molecular system. The balance between the V_3 and V_6 terms carry to the stabilized to the *staggered* form. The absolute values of V_3 and V_6 give the barrier energy and form, respectively.

NBO calculations were performed to explain the conformation of $CF_3SO_2CF_3$. It can be concluded that the anomeric effect tends to favor the *staggered* conformer.

IR and Raman spectra were obtained for $CF_3SO_2CF_3$, and 24 of the 27 expected normal modes of vibration were assigned. It was possible to scale the theoretical force field using the observed wavenumbers. The resulting SQM force field was used to calculate the potential-energy distribution, which revealed the physical nature of the molecular vibrations and the force constants in internal coordinates, which were similar to the values previously obtained for related chemical species.

Acknowledgments

The authors thank Consejo de Investigaciones de la Universidad Nacional de Tucumán (CIUNT), Consejo Nacional de Investigaciones Científicas y Técnicas, PIP 0629 (CONICET), Universidad Nacional de La Plata (UNLP) and Departamento de Ciencias Básicas de la Universidad Nacional de Luján (UNLu) for financial support. S.E.U and L.A.R.G especially thank Deutscher Akademischer Austauschdienst Germany (DAAD) for the FTIR spectrometer grant and financial support.

Appendix A. Supplementary data

Supplementary data associated with this article can be found, in the online version, at http://dx.doi.org/10.1016/j.saa.2012.05.049.

References

[1] (a) N.S. Simpkins, Sulphones in Organic Synthesis, Pergamon Press, Oxford, England, 1993;
(b) P.D. Magnus, Tetrahedron 33 (1977) 2019–2045.
[2] C. Najera, M. Jus, Tetrahedron 55 (1999) 10547–10658.
[3] N.S. Simpkins, Tetrahedron 46 (1990) 6951–6984.
[4] E.V. Hargittai, C.J. Nielsen, P. Klæboe, S. Ragnhild, J. Brunvoll, Acta Chem. Scand. A 37 (1983) 341–352.
[5] H. Oberhammer, G.D. Knerr, J.M. Shreeve, J. Mol. Struct. 82 (1982) 143–146.
[6] L.E. Fernández, A. Ben Altabef, E.L. Varetti, J. Mol. Struct. 612 (2002) 1–11.
[7] R.N. Haszeldine, J.M. Kidd, J. Chem. Soc. (1955) 2901–2910.
[8] M.E. Defonsi Lestard, L.A. Ramos, M.E. Tuttolomondo, S.E. Ulic, A. Ben Altabef, Vib. Spectrosc. 59 (2012) 40–46.
[9] M.J. Frisch, G.W. Trucks, H.B. Schlegel, G.E. Scuseria, M. Robb, A.J.R. Cheeseman, J.A. Montgomery Jr., T. Vreven, K.N. Kudin, J.C. Burant, J.M. Millam, S.S. Iyengar, J. Tomasi, V. Barone, B. Mennucci, M. Cossi, G. Scalmani, N. Rega, G.A. Petersson, H. Nakatsuji, M. Hada, M. Ehara, K. Toyota, R. Fukuda, J. Hasegawa, M. Ishida, T. Nakajima, Y. Honda, O. Kitao, H. Nakai, M. Klene, X. Li, J.E. Knox, H.P. Hratchian, J.B. Cross, V. Bakken, C. Adamo, J. Jaramillo, R. Gomperts, R.E. Stratmann, O. Yazyev, A.J. Austin, R. Cammi, C. Pomelli, J.W. Ochterski, P.Y. Ayala, K. Morokuma, G.A. Voth, P. Salvador, J.J. Dannenberg, V.G. Zakrzewski, S. Dapprich, A.D. Daniels, M.C. Strain, O. Farkas, D.K. Malick, A.D. Rabuck, K. Raghavachari, J.B. Foresman, J.V. Ortiz, Q. Cui, A.G. Baboul, S. Clifford, J. Cioslowski, B.B. Stefanov, G. Liu, A. Liashenko, P. Piskorz, I. Komaromi, R.L. Martin, D.J. Fox, T. Keith, M.A. Al-Laham, C.Y. Peng, A. Nanayakkara, M. Challacombe, P.M.W. Gill, B. Johnson, W. Chen, M.W. Wong, C. Gonzalez, J.A. Pople, Gaussian 03, Revision C.01, Gaussian, Inc., Wallingford, CT, 2004.
[10] R. Krishnan, J.S. Binkley, R.J. Seeger, J.A. Pople, J. Chem. Phys. 72 (1980) 650–654.
[11] A.D. Becke, J. Chem. Phys. 98 (1993) 5648–5652.
[12] C. Lee, W. Yang, R.G. Parr, Phys. Rev. B 37 (1988) 785.
[13] C. Alamo, V. Barone, J. Chem. Phys. 108 (1998) 664–675.
[14] W.J. Hehre, R. Ditchfield, J.A. Pople, J. Chem. Phys. 56 (1972) 2257–2261.
[15] P.C. Hariharan, J.A. Pople, Theor. Chim. Acta 28 (1973) 213–222.
[16] M.S. Gordon, Chem. Phys. Lett. 76 (1980) 163–168.
[17] D. McLean, G.S. Chandler, J. Chem. Phys. 72 (1980) 5639–5648.
[18] J.P. Perdew, K. Burke, M. Ernzerhof, Phys. Rev. Lett., 77 (1996) 3865-368; Erratum: Phys. Rev. Lett., 78 (1997) 1396.
[19] C.M. Møller, S. Plesset, Phys. Rev. 46 (1934) 618–622.
[20] M. Hargittai, I. Hargittai, J. Mol. Struct. 20 (1974) 283–292.
[21] E.D. Gledening, J.K. Badenhoop, A.D. Reed, J.E. Carpenter, F.F. Weinhold, Theoretical Chemistry Institute, University of Wisconsin, Madison, WI, 1996.
[22] P. Pulay, G. Fogarasi, G. Pongor, J.E. Boggs, A. Braga, J. Am. Chem. Soc. 105 (1983) 7037–7047.
[23] W.B. Collier, Program FCARTP (QCPE #631), Department of Chemistry, Oral Roberts University, Tulsa, OK, 1992.
[24] B. Nielsen, A.J. Holder, GaussView, User's Reference, Gaussian Inc., Pittsburgh, PA, 1997.
[25] J.L. Duncan, Mol. Phys. 28 (1974) 1177–1191.
[26] S. Millefiori, A. Alparone, J. Chem. Soc. Faraday Trans. 94 (1998) 25–32.
[27] L. Radom, W.L. Hehre, J.A. Pople, J. Am. Chem. Soc. 94 (1972) 2371–2381.
[28] L. Radom, J.A. Pople, J. Am. Chem. Soc. 92 (1970) 4786–4795.
[29] D. Bond, P.V. Schleye, J. Org. Chem. 55 (1990) 1003–1013.
[30] G. Fogarasi, X. Zhou, P.W. Taylor, J.A. Pulay, J. Am. Chem. Soc. 114 (1992) 8191–8201.